



Double Loop Decoupled Proportional Controller for Dynamic and Kinematic Model for a Ground

Bulbul Behera¹, Mohd. Imran Ansari², F.B. Sayyad² and S.F. Sayyad³

¹Department of Mechanical Engineering (Robotics), Defence Institute of Advanced Technology (DIAT), Pune, India

²Department of Mechanical Engineering, Dr D.Y. Patil School of Engineering, Lohegaon, Pune, India

³Department of Computer Engineering, AISSMS College of Engineering, Pune, India

(Corresponding author: F.B. Sayyad)

(Received 03 May 2019, Revised 10 July 2019 Accepted 17 July 2019)

(Published by Research Trend, Website: www.researchtrend.net)

ABSTRACT: In this paper the design of proportional controller has been described for tracking the heading angle of vehicle. A linear "Bicycle dynamic model" that takes into accounts the slip angle and ground wheel interaction has been used. The heading angle is same as the steering of front wheel so actuator dynamics was included in this model. The actuator dynamics and vehicle transfer function loops were decoupled to minimise the error and maximise accuracy of the system. Speed of the vehicle was influenced by the change of heading angle due to change in steering angle and velocity of vehicle So in this paper whole system was simulate for different velocity and controller gain. The result of simulation for both the dynamic and kinematic model with actuator dynamics and without actuator dynamics has been compared by using Matlab-simulink. Mathematical expression for the vehicle and actuator dynamics has been explained clearly. From the result of simulation it is found that the desired heading angle of 20 degree can be achieved in 2 seconds while the speed of vehicle is 4m/sec by tuning the controller effectively. A realistic mathematical model of the vehicle considering cornering stiffness was calculated by Hewson's method.

Keywords: Vehicle heading angle, proportional controller, kinematic model, dynamic model, cornering stiffness.

NOMENCLATURE

m : mass of the vehicle
Iz : yaw moment of inertia of the vehicle
 δ : steering angle of the front wheel
r : yaw rate of the vehicle
 θ : vehicle yaw angle measured with respect to the inertial global X-axis
v : velocity of the vehicle
Fyf : lateral tire force on the front wheel
Fyr : lateral tire force on the rear wheel
l : wheelbase
lf : distance of front tire from vehicle CG
lr : distance of rear tire from vehicle CG
Cf : cornering stiffness of the front wheel
Cr : cornering stiffness of the rear wheel

I. INTRODUCTION

An eloquent task in designing a controller for a ground vehicle is a challenge. In this paper the heading angle is controlled by a proportional controller with K_p 0.08 with 2% of overshoot. The dawn of motor vehicle age occurred around 1769 when the French military engineer, Nicholas Joseph (1725-1804), built a wheel wheeled stream driver vehicle for the purpose of pulling artillery pieces [1, 2]. With higher speed the vehicle dynamics of the vehicle particularly turning and braking assumed greater importance as an engineering concern. A car with "over steering" the driver's hand pushes towards greater steer angle [3]. This paper focused on rubber tire vehicle. The vehicle motion accomplished in accelerating, braking (deceleration), cornering and ride is a response of force imposed. On March 13, 2004 a gaggle of engineers congregated outside a California dive bar to watch 15 self driving cars in the first ever DARPA (Defence Advance Research Project Agency) grand challenge. The first big push towards a fully autonomous vehicle.

It bridges the gap between fundamental discourtesies and military uses. All the self driven vehicle was need to cross the 250 km (150 miles) in a limited time. No vehicle able to finished, in fact no vehicle able to finish 150km (7.3 miles) most vehicle died all together. Carnegie Mellon University's self driving vehicle "Sandstorm" travelled the farthest distance, completed 11.78 km (7.32 miles), it used pursuit algorithm based on geometric method of path follow. On October 28, 2005 second DARPA grand challenge was scheduled 23 self driven vehicles surpassed the 11.78 km distance completed by the best vehicle in 2004. Stanley vehicle completed the challenge in 6h: 54 min; vehicle passed through 3 narrow tunnels and negotiated more than 100 sharp left and right turns. This vehicle used a steering control law based on kinematic bicycle model. In 27 DARPA urban challenges "Boss" own the challenge in less than 5 hour to complete the 96 km urban race-course used predictive control strategy.

This leads automotive dynamics engross the study of how and why the forces are generated. The ascendant forces acting on the system to control process are generated by the tire against the road. Understanding the vehicle dynamic can accomplished by the two levels, that is the empirical and analytical. The empirical understanding derives from trial and error method. This sometimes led to failure at some other value of controller gain. It might be noted analytical method also are not foolproof because they usually only approximate reality. In this study considering the mathematical modelling and system identification to determine the vehicle dynamic in section III.

The vehicle is consisting of many components arranged in its exterior envelope. For example when brake the vehicle slow down so it can be presented as one lumped mass located at its centre of gravity (CG) with appropriate mass and inertia property.

It is often necessary to treat wheels as different lumped masses. The mass of the vehicle usually referred to as “sprung mass” whereas the mass of the running gear together with associated components referred as “unsprung mass”. In this paper consider two degree of freedom that is lateral motion y and heading angle θ . Take into account both the kinematic and dynamic model. Only front wheel of the vehicle is steerable, the dynamic analysis is based on “dynamic bicycle model” [4]. The vehicle is turning to the left shown in the Fig. 2.

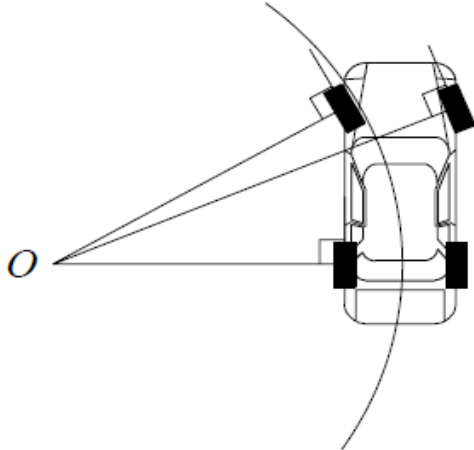


Fig. 1. Steering length of high speed vehicle.

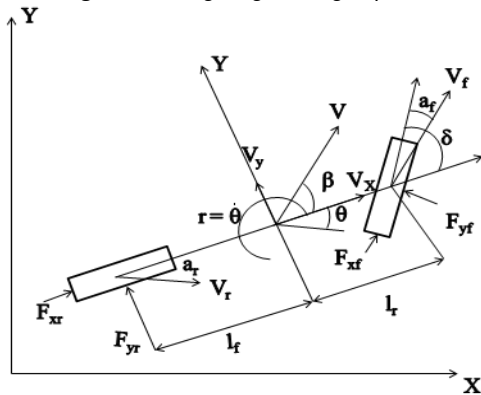


Fig. 2. Dynamic bicycle model.

Several types of control algorithm are available to control the system depended on mission purpose. The mission plan is consisting of navigation algorithm that determines heading angle based on steering of front wheel. Here the concern is controlling the heading angle of a vehicle to maintain its continuous movement. The problem is controlling the heading angle in real environment. The controller model simulated for 4 m/s, 10 m/s and 20 m/s. The system is decoupled into two loops and cascaded. The inner loop control the steering actuator while the outer loop is controlling the heading angle whereas the input is steering angle. When the vehicle's velocity is very low, there is a condition between the inner wheel and outer wheel that allows them to turn slip-free, is called kinematic condition [5-7]. The condition is called “Ackerman” condition. If inner wheel of the vehicle with high velocity must actuate at a lower steer angle than the kinematic steering.

The kinematic system response can be calculated simply by dividing velocity (V) by wheelbase (l). When the velocity of vehicle is very low there is no centrifugal. As the velocity increases centrifugal force act significantly and this leads to change the circular motion. As velocity

increase the K_p value will be decreases. The change in K_p value is very small. Cornering stiffness is estimated on the basis of tyre basic parameter. Although it is difficult to get highly accurate as it is calculated on simple parameter value. But it provides a process for calculating the heading angle of vehicle somewhat it will be manageable. So in this work cornering stiffness was calculated by both vertical load and from basic tyre information. In this work a proportional controller has been implemented to control the vehicle heading angle when the input to this system is steering angle with actuator dynamic discussed in section III. The response of the dynamic model with over steered is simulated in Matlab-simulink [8] and compared with the kinematic model when vehicle is travelling at a rate of 4m/second.

III. METHODOLOGIES OF VEHICLE DYNAMIC ANALYSIS OF SYSTEM

A simple approximation of the lateral dynamics of land vehicle is that the “bicycle model” [7]. This approximation combines the results of the two front wheels and treats them as a one wheel. The bicycle model conjointly combines the 2 rear wheels and treats them as united wheel.

The bicycle model considered in this study with two degree of freedom is shown in the Fig. 1. The two degree of freedom are vehicle yaw angle θ and vehicle lateral motion y . The vehicle lateral position is measured on the lateral axis of the vehicle and therefore the vehicle yaw angle is measured with relevance the world coordinate axis. The lateral force at the tire-road interface depends on the slip angle. It is assumed that solely front wheel is manageable (steerable).

Lateral motion of the vehicle is described by

$$m\dot{v}_y = F_{xf} \sin \delta + F_{yf} \cos \delta + F_{yr} \quad (1)$$

The equation for the yaw motion is

$$I_f \dot{\theta} = l_f F_{xf} \sin \delta + l_f F_{yf} \cos \delta - l_r F_{yr} \quad (2)$$

Considering δ to be very small, (1) and (2) can be written as

$$m a_y = F_{yf} + F_{yr} \quad (3)$$

$$I_f \dot{\theta} = l_f F_{yf} - l_r F_{yr} \quad (4)$$

The velocity vector v can be written as

$$V = v_x i + v_y j \quad (5)$$

Where, i and j are the unit vector in x and y directions respectively, here v_x and v_y are the velocity vector in x and y direction respectively. The x - y coordinate system is fixed to the vehicle. The should be written as

$$A = (v_x - v_y r) i + (v_y + v_x r) j \quad (6)$$

Substituting y -value of the equation (6) into (3), the lateral motion of the vehicle is described by

$$m(\dot{v}_y + v_x r) = F_{yf} + F_{yr} \quad (7)$$

Progressive revenues convince deviate in that how the lateral tire force of a tire is proportional to the slip-angle for very small slip-angles.

The slip angle of a tire is outlined because the angle between the orientation of the tyre and also the orientation of the velocity vector of the wheel as shown in Fig. 3.

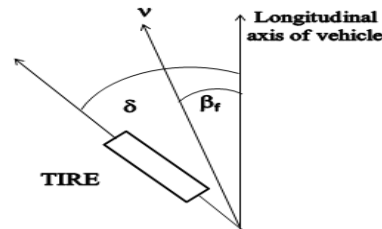


Fig. 3. Tire slip angle.

The slip angle of front and rear wheels is

$$a_f = \delta - \beta_f \quad (8)$$

$$a_r = -\beta_r \quad (9)$$

Where, β_f and β_r are the angles that the velocity vectors of the front and rear wheels make with the y axis of the vehicle respectively. When a side-slip angle is negative, F_{yf} and F_{yr} act in the positive y-direction. For small slip angles, the lateral forces acting potent on the function (front) and service (rear) wheels can be written as

$$F_{yf} = C_f a_f \quad (10)$$

$$F_{yr} = C_r a_r \quad (11)$$

$$m\dot{v}_y + \left(\frac{C_f + C_r}{v_x}\right)v_y + \left(mv_x + \frac{C_f l_f - C_r l_r}{v_x}\right)r = C_f \delta \quad (12)$$

$$I_z \dot{r} + \left(\frac{C_f l_f - C_r l_r}{v_x}\right)v_y + \left(\frac{C_f l_f^2 + C_r l_r^2}{v_x}\right)r = C_f l_f \delta \quad (13)$$

Now rearranging Eq. (14) and (15), the state space model can be written as

$$\begin{bmatrix} \dot{v}_y \\ \dot{r} \end{bmatrix} = \begin{bmatrix} -\frac{C_f + C_r}{m v_x} & -v_x - \frac{C_f l_f - C_r l_r}{m v_x} \\ -\frac{C_f l_f - C_r l_r}{I_z v_x} & -\frac{C_f l_f^2 + C_r l_r^2}{I_z v_x} \end{bmatrix} \begin{bmatrix} v_y \\ r \end{bmatrix} + \begin{bmatrix} \frac{C_f}{m} \\ \frac{C_f l_f}{I_z} \end{bmatrix} \delta \quad (14)$$

The transfer function is given by

$$G_\delta^r(s) = \frac{a_{r1}s + a_{r2}}{s^2 + 2\xi\omega_n s + \omega_n^2} \quad (15)$$

Where as $a_{r1} = \frac{C_f l_f}{I_z}$ and $a_{r2} = \frac{C_f C_r l}{m I_z v_x}$

$$2\xi\omega_n = \frac{m(C_f l_f^2 + C_r l_r^2) + I_z(C_f + C_r)}{m I_z v_x}$$

and $\omega_n^2 = \frac{C_f C_r l^2}{m I_z v_x^2} - \frac{(C_f l_f - C_r l_r)}{I_z}$

The transfer function $G_\delta^\theta(s)$, which is the response of heading angle to steering angle, is obtained as

$$G_\delta^\theta(s) = \frac{a_{r1}s + a_{r2}}{s(s^2 + 2\xi\omega_n s + \omega_n^2)} \quad (16)$$

A. Modelling of Steering Actuator

In order to keep the vehicle heading angle, the steering wheels of the ground vehicle ought to follow the command signals received from the vehicle controller and prolong synchronization with the steering motor. Associate acceptable actuator mechanism model has to be established. Therefore, the transfer function model is springs analytically from the electrical and mechanical governing equations of the motor that is obtained from initial principles. To model the steering actuator, visualization as shown in Fig. 4, is taken into account. The governing equations supports on the Newton's law combined with the Kirchhoff's law.

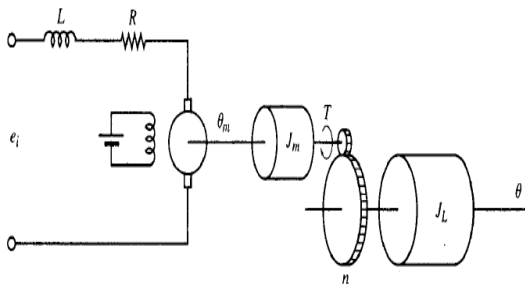


Fig. 4. Semantic diagram of steering actuator.

The torque generated by the motor is T . The moment of inertia of the motor rotor is J_m . The angular displacements of the motor rotor and the load element are θ_m , and θ respectively. The equation for torque equilibrium is given by;

$$J \frac{d^2\theta}{dt^2} + b \frac{d\theta}{dt} = T \quad (17)$$

$$\text{and } Ri + L \frac{di}{dt} = V - V_b \quad (18)$$

Applying the Laplace transform to (17) and (18), the transfer function, that makes relation between the angle of rotation of the steering actuator, $\theta(s)$, to the input voltage, $V(s)$, is obtained as

$$G_\delta^\theta(s) = \frac{1}{s} \left(\frac{K_t}{(Ls + R)(Js + b)K_t + K_b} \right) \quad (19)$$

A DC motor has taken with a 156:1 reduction gear ratio to control the heading angle. It is attached to the steering shaft by means of spur gear with a reduction ratio of 1.47. The standard rack and pinion steering system of the vehicle has a gear ration of 15.5. So the gearing ratio between the front wheel and steering shaft is $156 * 1.47 * 15.5 = 3554.46$.

Table 1: Parameter of Steering Actuator.

Parameter	Value	Unit
Terminal Resistance (R)	0.317	Ohms
Terminal Inductance (L)	0.0823	mH
Torque constant (K_t)	30.2	mNm/A
Speed constant	317	rpm/V
Back emf constant (K_b)	0.0301	V/rad/sec
Rotor inertia (J)	138	g.cm ²
Speed/torque gradient	3.33	rpm/mNm
Nominal speed (N)	6930	Rpm
Nominal torque 9 (T)	170	MNm
Nominal voltage (V)	24	V

By substituting the values from Table 1, in eq. (19) the transfer function G_δ^θ is obtained as

$$G_\delta^\theta = \frac{302}{s(0.044s + 9.164)} \quad (20)$$

B. System Parameter Identification

The dynamic bicycle model has some parameters that cannot be measureable directly. Although, by using some commonly available tools as a functional estimation can be done. So, the total mass of the vehicle, the C.G. location and the moment of inertia were estimated by using the vehicle's split mass, by using four aligning scales beneath each wheel. Sum of estimated mass of each wheel constitute the total mass of the vehicle and denoted as

$$M = m_{fl} + m_{fr} + m_{rl} + m_{rr} \quad (21)$$

where, m_{fl} , m_{fr} , m_{rl} , and m_{rr} are the mass of the vehicle at front-left, front-right, rear-left and rear-right respectively. Front and rear wheels are together considered as one wheel at the middle point of the axle respectively. The front wheel mass, m_f , and the rear wheel mass, m_r , are given by

$$m_f = m_{fl} + m_{fr} \text{ and } m_r = m_{rl} + m_{rr} \quad (22)$$

From this and a measurement of the wheel base l , the location of the vehicle's C.G., described by distances l_f and l_r from the front and rear axles along the centre line is obtained as

$$l_f = l \left(1 - \frac{m_r}{m}\right) \text{ and } l_r = l \left(1 - \frac{m_f}{m}\right) \quad (23)$$

Moment of inertia of vehicle is estimated by considering the vehicle as two point masses connected by a mass less rod. The moment of inertia for the vehicle is given by

$$I_z = m l_f^2 + m l_r^2 \quad (24)$$

The model transfer function depends on both physical and dynamic parameters. Vehicle parameters are listed below in Table 2.

By substituting the values from Table 2 in eq. (18) model transfer function G_s^θ is obtained by using over steered cornering stiffness parameter.

$$G_s^\theta(s) = \frac{232.227s + 9819.75}{s(s^2 + 131.87s + 3667.68)} \quad (25)$$

Table 2: Vehicle Parameters.

Parameter	Value	Unit
Mass of front-left wheel (m_{fl})	158	Kg
Mass of front-right wheel (m_{fr})	137	Kg
Mass of rear-left wheel (m_{rl})	360	Kg
Mass of rear-right wheel (m_{rr})	269	Kg
Mass of vehicle (m)	924	Kg
Wheel base (l)	1.93	M
Location of CG from front axle (l_f)	1.31	M
Location of CG from rear axle (l_r)	0.62	M
Moment of inertia (I_z)	748	Kg.m ²

IV. CONTROLLER FOR DESIRED HEADING ANGLE

Take into account a closed-loop negative feedback system for tracing the yaw angle as shown in Fig. 4. For this model the actual heading angle of the vehicle is the output. Input to the vehicle is steering angle depends on the desired heading angle for the required velocity of the vehicle. To steering the front wheel 20 degree, the front wheel takes time around 3 second and the vehicle heading angle response is as same as steering response, so the steering actuator model has been included in this study. The controller designed for this system is dissociated into two loops [9]. The inner loop controller, controls the desired and current rotation of the steering motor. The outer loop controller reduces the error between the desired and actual heading angles of the vehicle.

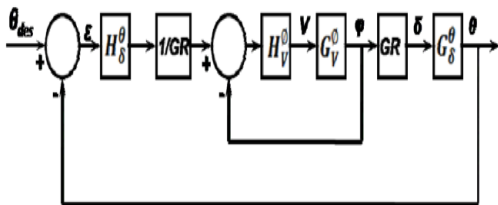


Fig. 5. Negative feedback system for desired heading angle with actuator.

A. Proportional controller

Consider the proportional heading angle controller

$$H_s^\theta = K_p$$

The maximum requirement of 2% over shoot results damping ratio ζ to be 0.6, with settling the time of 2s. The characteristic equation of vehicle is

$$S^3 + 131.87s^2 + 3899.907s + 9819.75K_p = 0$$

To understand the system response and to reduce the settling time the heading angle tracing response has been simulated by using Matlab-simulink considering without actuator dynamics and with actuator dynamics and found that K_p value 0.8 has satisfied the requirement.

V. KINEMATIC MODEL VEHICLE

The wheel kinematic constraints are moves on a horizontal plane, point contact on wheel, wheel not deformed, no slip, skid and no friction around the point contact.

The velocity of vehicle is very low $V \approx 0$. Centrifugal force does not act on the vehicle, lateral forces are not needed and no side slip angle is produced as the both front and rear wheels are travelling in heading direction and make a circular motion. Then the yaw rate is given by

$$r_s = \frac{V}{L} \delta \quad (26)$$

The actual steering angle of the front right and front left is not δ and little smaller for front left and larger for front right wheel.

$$\delta < 1 \quad (27)$$

So, δ can be neglected as it is, too smaller for front of the left wheel. The velocity of vehicle increases centrifugal force act significantly and centrifugal force act at the vehicle centre of gravity as shown in Fig. 6. So it is cleared that centrifugal force changes with speed which results side-slip angle to change, which is turn change the circular motion.

VI. ESTIMATING CORNERING STIFFNESS FROM BASIC TIRE INFORMATION

A tyre is orientated at an angle not equal to its direction of motion, a side force acts perpendicular to the plane of the wheel. The relation is nearly linear for small slip angles. The relationship that defines side force as a function of slip angle makes use of the tire cornering stiffness. The sidewalls are assumed to be negligibly stiff in the lateral direction, and hence their influence on the lateral dynamics of the tyre will be ignored. The resulting model is estimated to yield cornering stiffness values within about 30 percent of the actual measured values. Inevitable information such as wheel radius, tyre width, aspect ratio (which is ratio of tyre section height to tyre width) load index, type of tyre construction, maximum allowed inflation pressure on the tyre side walls need to be provided by the tire manufacturer. The cornering stiffness can be calculated by using a mathematical tire model, which is by using basic tire information [10]. The final expression proposed by Hewson to calculate cornering stiffness C_a is

$$C_a = \frac{8EbW^3}{L[2\pi(r_w + wa) - L]} \quad (28)$$

$$L = 2(r_w + wa) \sin[\cos^{-1}(1 - \frac{swa}{r_w + wa})] \quad (29)$$

Where E is the belt compression modulus, b is the tire belt thickness, r_w is the wheel radius, w is the belt width, a is the tire aspect ratio (tire section height/tire section width), L is the contact patch length and s is the unitized percent of sidewall vertical deflection when loaded. The parameters of tyre are listed in Table 3.

Table 3: Parameter of Tire.

Parameter	Value	Unit
Tire aspect ratio (a)	0.5	-
Tire belt thickness (b)	0.015	m
Belt compression modulus(E)	27e6	N/m ²
Wheel radius(r_w)	0.254	m
Unitized percent of sidewall vertical deflection when loaded(s)	15%	-
Belt width(w)	0.205	m

By using values of the tire parameters from Table 3 in eqn (28) and (29), the tire cornering stiffness is acquired as 132600 N/rad. As we are considering all four tires have same specification, in paper so the front and rare tires will have same value.

Table 4: Cornering Stiffness of Tire.

Estimated method	Cornering stiffness	Value (N/rad)	Under steer Co-efficient
From vertical load	Front tire C_{FN}	50000	$K_{US}=0$ (NS)
	Rare tire C_{RN}	106100	
Hewson method	Front tire C_{FO}	132600	$K_{US}<0$ (OS)
	Rare tire C_{RO}	132600	

The predicted data for the cornering stiffness of the wheel from Hewson's method are presented in Table 4. It is conventional to neglect the shear force when the length to width ratio increases 5:1 because with such a ratio error introduce is less than 5percent.

VII. RESULTS

The control system has been tested for tracing a step input of 20 degree heading angle with 1 maximum overshoot and a settling time less than 2 second. The longitudinal speed of the vehicle has been retaining a constant value of 4 m/second.

Here dynamic model is compared with the kinematic model. The damping ratio ζ is less than 0.6 where as setting time is 2 second. The yaw angle response has been simulated in Matlab-simulink for both the dynamic and kinematic model. Several experiments have been done in Matlab-simulink, to check the proportional controller gain (K_p) and it was found to be 0.8 without any overshoot when the vehicle is travelling with a constant speed of 4m/second. Simulation result has been shown in below Fig. 6.

For actuator dynamics, added a saturation block to limit the voltage -20 to +20 for the purpose of simulation. For a desired heading angle of 20 degree, the highest input steering angle was found to be 25 degree, which is within the steering limit of 35 degree. In this paper simulation has been done for different values of proportional controller gain (K_p).

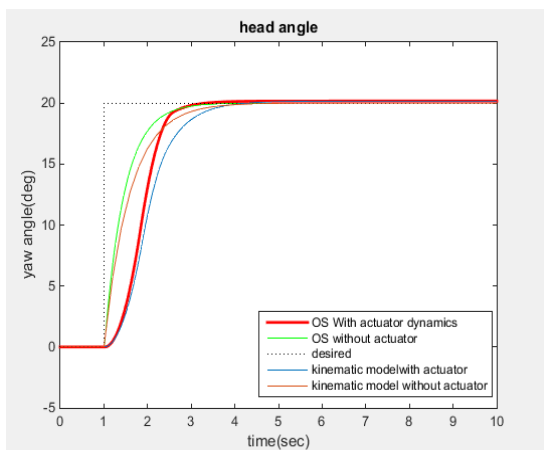


Fig. 6. Comparison of with actuator and without actuator for heading angle response with $K_p=0.8$.

From the simulated result it is cleared that the error between the desired and simulated result is 1.8 and 0.8

without actuator dynamics and with actuator dynamics respectively. So it is found from this the vehicle is in good condition when the actuator dynamics is added.

From the steering angle simulated result that is Fig. 7, for heading angle of 20 degree the steering angle for over steered without actuator and kinematic model without actuator is 15.9 and 16 degree respectively. Whereas, in case of over steered with actuator and kinematic model with actuator is 8.5 and 9 degree respectively. So without actuator dynamics practically it is unrealizable.

From the steering angle simulation result for $K_p=0.8$, it is cleared that there is sudden rise in steering angle when actuator model is not considered which is practically not possible. The steering angle reaches 16 degree without actuator. From this simulation result it is concluded that when velocity increase the proportional controller gain decreases.

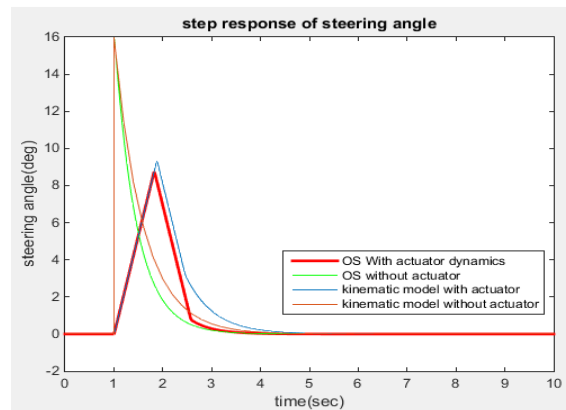


Fig. 7. Comparison of with actuator and without actuator for step response of steering actuator for 20 degree heading angle with $K_p=0.8$.

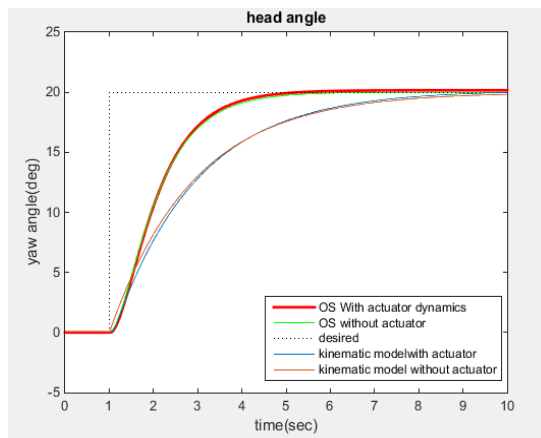


Fig. 8. Comparison of with actuator and without actuator for heading angle response for $K_p=0.1$ with velocity 10m/sec.

The velocity of vehicle increased to 10m/s, the controller gain decrease to 0.1. For the heading angle of 20 degree steering angle is found to be 1.8 degree for dynamic model with actuator and without actuator respectively.

Whereas for same heading angle of 20 degree the steering angle is found to be 1.98 and 2 degree for kinematic model with actuator and without actuator respectively. So it is found that from simulation results when velocity increases steering angle decreases.

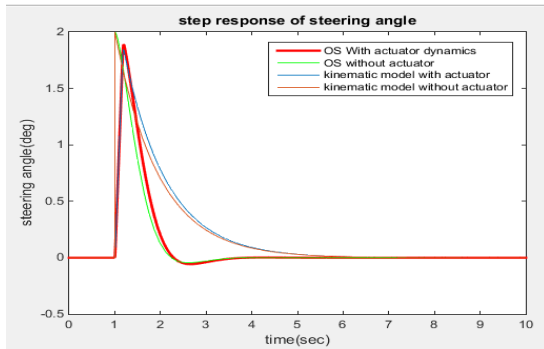


Fig. 9. Comparison of with actuator and without actuator for step response of steering actuator for 20 degree heading angle with $K_p=0.1$ with velocity 10m/sec.

Steering angle decreases with increase in velocity. When vehicle is moving with very high speed that is 10m/sec 1.8 degree of steering, heading angle reaches up to 20 degree which is within the steering limit.

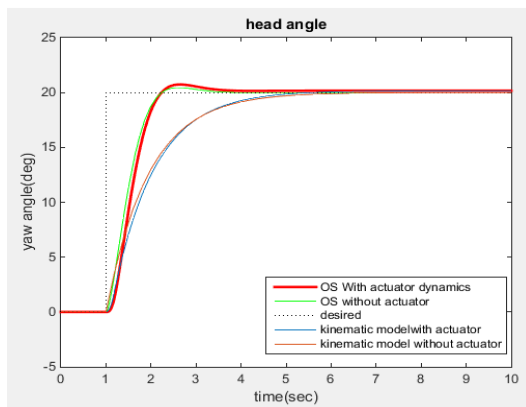


Fig.10. Comparison of with actuator and without actuator for heading angle response for $K_p=0.08$ with velocity 20m/sec.

When the vehicle is travelling with a velocity of 20m/s the controller gain again decreases to 0.08. With a steering angle of 0.5 heading angle reaches up to 20 degree. Whereas for kinematic model steering angle of 2 degree heading angle reaches up to 2 degree.

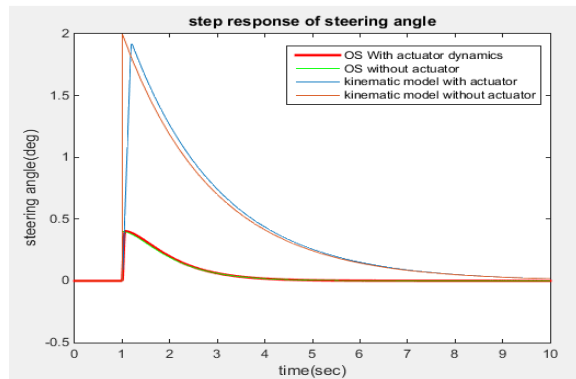


Fig. 11. Comparison of with actuator and without actuator for step response of steering actuator for 20 degree heading angle with $K_p=0.08$ with velocity 20m/sec.

VIII. CONCLUSION AND FUTURE WORK

In this paper, the design, analysis and turning of controller considering the “dynamic bicycle model”. The design parameter has also been studied by mathematical analysis with simulated in Matlab-simulink. The vehicle controller is dissociated into two loops, the internal loop controller, controls the inaccuracy between the desired and current rotation of steering actuator and the input to this loop is a function of steering angle that is calculated based on the error in heading angle of the vehicle. The exterior loop of the controller reduces the inaccuracy between the desired and actual heading angle. The time taken to steer the front wheel to reach 20 degree is around 3second and same as response time of the heading angle which is in the steering limit of 30 degree, the steering actuator has been included in this experiment.

When the velocity of the vehicle is 4m/sec to reach 20degree heading angle it takes 2seconds with steady state error that is less than 5%.When controller gain increases there is a sudden rise in the steering angle. And 20 degree of steering angle produces 20 degree of heading angle which is not possible in practically, so actuator dynamics is need for vehicle dynamics. In this work dynamic model and kinematic model was compared. When the velocity of vehicle is very slow in that condition, kinematic condition arises. The whole mathematical analysis of dynamic model, that is converting the forces and the inertia equation of bicycle model to state space and then state space to transfer function of heading angle to steering angle that is $G_{\delta}^{\theta}(s)$ can be replaced by kinematic model, simply by replacing the transfer function block by “V/L”. From the simulated result it is concluded that when vehicle is moving with very high speed, with very low steering angle the heading angle of vehicle reaches up to 20 degree. In kinematic model settling time is more than the dynamic model. However, these analyses in a kinematic model settling in time are inspiring us to follow in near future with the help of various optimization techniques for reducing the error and improve the vehicle consistency.

ACKNOWLEDGEMENT

Authors' wish to thanks Dr D G Thakur (Professor), DIAT-DRDO, Pune and Dr. D K Singh (Professor & Head), MMMUT, Gorakhpur for necessary support and help.

REFERENCES

- [1]. Gillespie, T.D., (1992). Fundamentals of Vehicle Dynamics. *Society of Automotive Engineers*, Warrendale.
- [2]. Sahoo, S., Shubharamanian, S.C., Srivastava, S., (2016). Evaluation of the transient response and implementation of a heading-angle controller for an autonomous ground vehicle. *Proceedings of the Institution of Mechanical Engineers, Part D: Journal of Automobile Engineering*, Vol. **230**(8): 1040-1056.
- [3]. Sahoo, S., Subramanian, S. C., Mahale, N., Srivastava, S., (2015). Design and development of a heading angle controller for an unmanned ground vehicle. *International Journal of Automotive Technology*, Vol. **15**(1): 27-37.
- [4]. Wong, J.Y., (2002). *Theory of ground vehicle* 4th edn. Wiley, New York.

- [5]. Koenig, S., Likhachev, M., (2002). Improved fast replanning for robot navigation in unknown terrain," *Proceedings of the IEEE International Conference on Robotics and Automation (ICRA)*, May:968-975.
- [6]. Morin, P., Samson, C. (2009). Control of nonholonomic mobile robots based on the transverse function approach. *IEEE Transactions on Robotics*, Vol. **25**(5): 1058-1073.
- [7]. Jazar, R.N. (2008). Vehicle dynamics: Theory and application. *Springer-Verlag New York*.
- [8]. Singh, A. K., Saxena, A., Gupta, M., (2017). Study and analysis of use of mechatronics in modern machine design" *International Journal on Emerging Technologies (Special Issue NCESTST)*, Vol. **8**(1): 345-354.
- [9]. Suppachai, H., Silawatchananai, C., Parnichkun, M., Wuthishuwong, C. (2009). Double loop controller design for the vehicle's heading control. *Proceedings of the IEEE International Conference on Robotics and Biomimetics*, 989-994.
- [10]. Sahoo, S., Subramanian, S.C. and Srivastava, S. (2014). Sensitivity analysis of vehicle parameter for heading angle control of an unmanned ground vehicle. *ASME International Mechanical Engineering Congress and Exposition*, Vol. **12**: 14-24.

How to cite this article: Behera, B., Ansari, M.I., Sayyad, F.B. and Sayyad, S.F. (2019). Double Loop Decoupled Proportional Controller for Dynamic and Kinematic Model for a Ground. *International Journal on Emerging Technologies*, **10**(2): 129-135.